

VALIDATING A TOVS CLOUD CLEARING SCHEME USING AVHRR DATA

P.D.Watts and J.R.Eyre

Meteorological Office Unit,
Robert Hooke Institute for Cooperative Atmospheric Research,
Clarendon Laboratory, Oxford, U.K.

1. INTRODUCTION

A new cloud clearing scheme is undergoing operational trials in the Local Area Sounding System of the U.K. Meteorological Office. Prior to these trials a sensitive method of validation of the cloud clearing of HIRS (High-resolution Infra-red Radiation Sounder) radiances was devised using AVHRR (Advanced Very High Resolution Radiometer) data. With this method of validation, the performance of the new cloud clearing can be compared with that of the existing scheme. Many interesting features of cloud clearing infra-red radiances become apparent when an accurate "ground truth" is available; normally the error characteristics of the cleared radiances are obscured by larger errors inherent in the validation system. The new cloud clearing scheme and the operational scheme which it is intended to replace are only described briefly here. A summary of the approach used in the new scheme is given by Eyre et al. (1985) and full descriptions of both schemes are available elsewhere (Eyre and Watts 1986, Watts 1985). The Local Area Sounding System is described by Eyre (1984).

2. NEW AND OLD CLOUD CLEARING SCHEMES

The new cloud clearing scheme (NCCS) is intended to improve upon and replace the version currently operational in the Local Area Sounding System (LASS). Hereafter in this paper any reference to "LASS" will be to the cloud clearing part of the operational scheme rather than to the processing suite as a whole.

NCCS is based on LASS and uses the same basic cloud detection mechanism. The Microwave Sounding Unit channel 2 (MSU-2) brightness temperature is estimated from HIRS brightness temperatures and compared to the measured value. If the two values are the same, to within a certain limit, the field of view (FOV) is assumed to be clear of cloud. A higher value in the measured brightness temperature indicates the presence of cloud. If this is the case, then an attempt is made to account for the effect of the cloud on the radiances using the adjacent field of view or N* method (Smith 1968). If this fails (for a variety of reasons), then, in the LASS scheme, the FOV is abandoned as too cloudy. At this stage the LASS cloud clearing is

essentially finished. In NCCS, if the N* method fails, linear combinations of the MSU channels (unaffected by cloud) are used to obtain estimates of the clear HIRS radiances. The coefficients for this process are obtained by multiple linear regression on theoretically computed TOVS brightness temperatures derived from a large set of radiosonde profiles. In NCCS, this cloud detection and correction is carried out on all FOVs rather than on only every second line and second FOV as in LASS. In this way NCCS establishes a complete field of HIRS and MSU data whereas the result of LASS is an intermittent field of data with large gaps in very cloudy areas. The "MSU regression" route in NCCS produces large areas of HIRS data which have locally correlated errors. The problem is sufficiently acute that an analysis scheme is included to estimate this error and subsequently account for it. In NCCS we consider that better estimates of the brightness temperatures are obtained by smoothing the field to a certain degree, i.e. by locally combining estimates. To do this optimally we require estimates of the errors in the brightness temperatures and a part of NCCS performs this estimation.

In summary, NCCS and LASS use the same cloud detection and correction mechanisms except in very cloudy areas where NCCS obtains clear HIRS values from the MSU. NCCS attempts to retain the full information content of the data by clearing on every FOV and includes a filter to use these data optimally. For more details on both schemes the above references should be consulted. The validation exercise reported here examines the following aspects of NCCS; its performance relative to LASS, the error characteristics of the various cloud clearing routes, and the behaviour of the filter and of the scheme for analysis of the bias in estimates obtained by the "MSU regression" route. regression bias analysis.

3. VALIDATION SCHEME USING AVHRR DATA

3.1 Rationale

It is possible to use AVHRR data to validate a TOVS cloud clearing scheme because AVHRR has infra-red channels (4 and 5) in the same (11 μ m) window region as HIRS channel 8. The latter can be readily synthesised from the former. Providing that the two instruments can be collocated to a sufficient accuracy (about 1 km) and that cloud contamination of AVHRR data can be identified with a high degree of certainty (about 1% error in detection of contaminated pixels), an estimate of the clear value of HIRS channel 8 can be obtained. One drawback of such a method is that relatively large amounts of AVHRR data have to be processed to validate a single pass of HIRS data, and the method is therefore only practicable for a limited number of passes. However, a large variety of cloud conditions are normally met within a single pass, thus providing a reasonably wide test of the scheme. Secondly, only HIRS window

channels can be synthesised from AVHRR and so the performance of the cloud clearing scheme for other channels remains untested. This is only a minor problem since HIRS window channels are the most sensitive to cloud effects. However, there are dangers in a scheme highlighting only one channel, and it may be over-sensitive to errors which would be negligible in most other channels. Finally, it is only where there are clear AVHRR pixels that a synthesised HIRS channel 8 can be obtained so that the method fails in very cloudy areas. This problem is unavoidable and is probably the only serious drawback in this method of validation.

An alternative and more conventional method is to use collocated radiosondes and to compute the radiances expected from the observed profiles. This has the advantages that all HIRS channels can be checked and there is no restriction to partly clear areas. However deficiencies in the radiative transfer model used, lack of surface temperature information in the sonde report and the space and time tolerances of the collocation criterion all introduce differences which will tend to mask the cloud clearing errors one is trying to observe. Retrieved temperature profiles can be compared (e.g. McMillin and Dean, 1982) but at the expense of introducing retrieval errors which can be more damaging to the comparison (Eyre and Watts 1986, Eyre 1987). It will be shown that a HIRS 8 value synthesised from AVHRR is accurate to about 0.3 K and therefore an order of magnitude better than that which might be expected from radiosonde collocations. It is also significantly less than typical cloud clearing errors (2-5 K) so that it provides an effective "ground truth" and thus allows quantitative conclusions to be drawn that would otherwise be impossible.

A significant advantage in using AVHRR is in the density of collocations available; a typical pass allows 50-70% of the HIRS FOVs to be validated. This is a very useful feature, as an important assumption of NCCS is that radiance fields can be expected to be horizontally consistent. Exactly how consistent (in channel 8) and how successfully the filter achieves this consistency can be seen using the AVHRR.

In summary, although the validation only applies directly to channel 8 and in regions with some clear areas, the high accuracy and density of collocations more than compensate for the drawbacks. The accuracy allows quantitative checks to be made on the cloud-cleared radiances and on the error estimates, and the high density allows detailed effects of the filter to be monitored.

3.2 Method

Details of the method of validation are given in Eyre and Watts (1986) but the main points and some supporting evidence for its validity are given here. The HIRS FOV is collocated with the AVHRR to

within 1 km (Aoki 1983; Lloyd et al. 1985) and the AVHRR pixels associated with each HIRS FOV are thus identified. Cloud contaminated pixels are identified using the scheme described by Saunders (1986), employing AVHRR channels 1, 2, 4 and 5 during the day and channels 3, 4 and 5 at night. AVHRR channels 4 and 5 and HIRS channel 8 all lie in the 11 μ m window region with the AVHRR channels lying either side of the HIRS; Figure 1 shows the spectral response functions of the three channels. Thus, values of AVHRR channels 4 and 5 averaged over the HIRS FOV can be used to estimate HIRS channel 8 (using a regression relation). Figure 2 shows the HIRS 8 value derived from AVHRR (hereafter called AVHRR"8") plotted against the measured HIRS 8 brightness temperature for all FOVs of a pass before cloud clearing, i.e. both AVHRR and HIRS data are cloud contaminated. The fit can be seen to be good, giving a bias of 0.2 K and a standard deviation of 0.3 K. The validation scheme utilises our ability to identify contaminated AVHRR pixels in order to average over the remaining clear pixels to obtain an AVHRR"8" which is an estimate of the clear HIRS 8. The accuracy of the clear AVHRR"8" is unlikely to be better than the figures quoted above, and may be degraded somewhat by residual contamination of the AVHRR. However, the cloud detection scheme was designed to find clear pixels and the number of cloudy pixels admitted is found to be very small. In fact, the number of clear pixels is usually underestimated. In summary we can expect the AVHRR"8" clear value to be no more than 0.4-0.5 K from the truth. By comparison, typical cloud clearing errors in HIRS 8 are around 2-5 K.

Figures 3a and 3b summarise the method for part of a pass of data (25 January 1986 at 1307Z). Figure 3a is AVHRR channel 2 (near infra-red) with collocated HIRS footprints overlaid. Figure 3b is the "cloud mask" and is grey or black for the pixels considered cloudy by the AVHRR detection scheme. The numbers above the ellipses give the AVHRR"8" values derived for the clear portion remaining (in tenths of a degree with the leading figure omitted, e.g. 784 = 278.4 K). Notice that no value is present for totally cloudy HIRS FOVs.

The symbols within the ellipses indicate the route by which NCCS obtained clear radiances. In brief, "." indicates that the FOV was judged clear, "*" indicates cloud clearance by the N* method and, apart from residual contamination checks "A" and "#", all other symbols indicate failure of the N* method for one of a variety of reasons (see Eyre and Watts 1986, or Watts 1985).

3.3 Histograms and statistics

Clear radiances are produced by both LASS and NCCS, and the resulting HIRS 8 value may be compared with the AVHRR"8". An instructive way to examine the differences is in the form of histograms. Figure 4 is an example of such a histogram for the NCCS scheme, and we now describe the notation in this and subsequent histograms. Positive values represent AVHRR"8" warm with respect to

HIRS 8. There are 1170 collocations with a standard deviation (S.D.) of 3.7 K and a bias of 1.6 K. In view of the accuracy of AVHRR "8" as a measure of the clear HIRS 8 temperature these differences may be regarded practically as errors in the cloud cleared HIRS 8 values. On each histogram a value of "P.E." is given. This is the mean value of the error estimated by the NCCS scheme itself and used in the sequential estimation filter. The above collocations may be split advantageously into subsets of the whole. Firstly the set of FOVs where LASS obtained clear radiances is selected in order to compare the relative performance of the two schemes. Other obvious subsets are the cloud clearing routes - clear, N* and MSU regression - with the further separation into land and sea areas also instructive.

4. SOME RESULTS

4.1 Comparison of NCCS with LASS

Figure 5a is the histogram of errors obtained with LASS for a pass at 1319Z on 16 April 1985. 154 collocations were obtained with a standard deviation of 3.5 K and a bias (HIRS cold) of 1.1 K. Over the same FOVs, Figures 5b and 5c show the errors obtained with NCCS at the pre- and post-filtered stages respectively. The standard deviations and biases are seen to be substantially lower than the LASS results. The filtering stage does not have a large impact in this case, reducing the standard deviation by only 0.2 K. Figures 6a and 6b are the error histograms for all NCCS collocations for the same pass, for pre- and post-filtered stages respectively. With cloudier situations included, the filter can be seen to be more effective, reducing the standard deviation by 1.0 K. The final standard deviation and bias of 3.0 and 0.4 K respectively are both lower than the results for LASS over its limited set. In general we may expect NCCS errors for all collocations to be larger than NCCS errors for the limited LASS set, since the former will include cloudier areas. However, in this case the performance is not greatly degraded over all FOVs.

In conclusion, NCCS performs better than LASS with respect to both standard deviation and bias of errors. Many more clear radiances are produced with NCCS in cloudier areas but they remain of a standard comparable to or better than LASS.

4.2 Error characteristics

The histogram in Figure 4 of unfiltered NCCS errors shows a spread of errors. It is very instructive to split the statistics into types of clearance and, in some cases, into land and sea areas. The typical error characteristics then become apparent.

Figure 7 is a histogram of the FOVs determined clear by NCCS from the same pass (1307Z, 25 January 1986) for both land and sea areas. There is a large peak value almost at zero difference which represents the genuine clear FOVs. At larger values of AVHRR⁸-HIRS 8 there is a decreasing "tail" of contaminated FOVs that have been passed as clear. The number in the "tail" at more than 2.0 K difference is quite large. This result was obtained with the improved NCCS, incorporating visible threshold and low cloud checks described in section 4.4. The length of the tail is related to any bias present in the estimated MSU-2 value used in the cloud detection (see Watts 1985 Appendix E). A warm bias in this value creates a longer tail. A cold bias would tend to remove the tail but increasingly at the expense of losing genuine clear FOVs. An attempt has been to identify and correct for a damaging warm bias in the estimated MSU-2 values and this is described in section 4.4. The above results, with a relatively short tail, were obtained after this bias correction had been applied.

The predicted errors for the clear FOVs are obtained from a knowledge of the limb-correction and radiometric errors and from the likely amounts of cloud missed because of the uncertainty in the estimated MSU-2 (Watts 1985 Appendix A). The resulting mean value of 2.0 K for this pass is close enough to the actual mean errors to have an appropriate effect in the filter.

Disregarding the very small number of "clear" FOVs which appear too warm (probably due to contamination in AVHRR), the error characteristics of "clear" FOVs are an edge at zero error with a tail of increasing cold error. The filter currently weights according to error variance, i.e. it assumes a normal distribution of errors with zero mean. The above error characteristics suggest a more suitable estimator should be used.

Figure 8 is the histogram of errors for "N*" FOVs for the same pass. The distribution of errors can be seen to be more nearly normal than that of the "clear" FOVs. The mean error is also reasonably near zero. Thus error characteristics of "N*" FOVs are well suited to the filter currently in NCCS. The error estimated for an N* clearance is calculated from expected errors in all the quantities used in its derivation and some assumptions about the correlation of these quantities. The average predicted value comes out far too high at 14.7 K compared to the actual mean value of 2.8 K. The result is that these FOVs get too little weight in the filter and some investigation of these predicted errors is described in section 4.4(f).

HIRS estimation by regression on MSU data is the third route to a set of clear radiances. Figures 9a and 9b are histograms of the MSU regression route for the same pass for land and sea FOVs respectively. As expected from a regression relation, locally consistent biases are apparent. The sea FOVs are particularly strongly biased by an average 8 K (HIRS cold) on this occasion. The standard deviations, however,

are reasonably small (around 2 K) and should represent the expected error in the filter if the bias correction part of the scheme is fully successful. The value of 6.2 K for the mean predicted error is simply the expected error from the regression and takes no account of the bias correction having removed part of it. However, we think it prudent to allow such a high value to remain because even after the bias correction the smaller errors remaining are likely to be locally correlated and therefore damaging if these data are weighted too heavily.

4.3 The effect of the filter

We have already shown in section 4.1 that the filter in NCCS is useful to some extent and now describe its behaviour in more detail. Figures 10a, 10b and 10c are histograms for all FOVs (for the same pass) for NCCS before filtering, after the bias correction has been made to the MSU regressions and after filtering respectively. It can be seen that the MSU bias correction is responsible for a large drop in the overall standard deviation (and bias), larger in fact than the filtering of the brightness temperature field. This is a common result mainly because "MSU regressions" constitute a large proportion of the clearances and because they are often badly biased. Because of the greater degree of genuine variation in brightness temperature over the land than over the sea filtering is less effective in the former case. Inspection of the histograms shows that the filter tends to remove outliers but fails to tighten the main peak. In general, when true variations in a field become equal in magnitude to the errors or noise which we are trying to remove, filtering improvements will be limited to removing "rogue data". The different characteristics of land and sea are accounted for by filtering less strongly over land (see section 4.4).

"Clear" FOVs have the lowest expected error and are usually the most accurate clearances in the field. They therefore usually supply other FOVs with information rather than receive it. Consequently, where they are inaccurate with a long cold "tail", not only can they be damaged themselves, but they can also damage other FOVs through the filtering process. The effect of the filter is to produce a peak in the new histogram towards the "centre of mass" of the tail in the unfiltered "clear" histogram. The standard deviation is reduced but there is also a detrimental effect on other FOVs.

"N*" FOVs, with normally distributed unbiased errors, are treated by the filter in a simple manner. They tend to remain unbiased and improve in accuracy. "N*" FOVs are used in the bias correction of "MSU regression" FOVs and their lack of bias is an important advantage here.

"MSU regression" FOVs have also quite normally distributed errors though commonly about a large bias. In an ideal case, the bias correction (which is performed through a filtering procedure) removes the bias and reduces the standard deviation. The filter then only has a minor effect on these FOVs because much of the information from adjacent "clear" and "N*" FOVs has gone into the bias correction. The bias correction to the "MSU regression" FOVs tends to be worst when it is based on neighbouring, supposedly "clear" FOVs which are in fact too cold.

In summary, the filter is shown to be very useful in reducing errors in channel 8 brightness temperatures (and therefore by implication in all other channels). There are two parts to the filter: the MSU regression bias correction and the filtering of the final fields. The bias correction is very important for channel 8 but may become less so for channels with higher peaking weighting functions, for which the regression relation between the HIRS and MSU is stronger. The brightness temperature filter works well over the sea and less well over the land where genuine variations are larger. For channels peaking higher than HIRS 8 we may expect that genuine variations in the field will become much less than the cloud-clearing noise and thus the filter should be still more effective. A danger of the filter is that it not only allows good unbiased information to be used optimally but it also allows biased information to corrupt the good. The cold tail for "clear" FOVs is an example and efforts should be (and have been) made to reduce it.

4.4 Improvements made to NCCS

This section describes changes made recently to NCCS mainly as a result of findings from the validation exercises.

(a) Filtering strengths.

Detailed inspection of images like Figure 3a reveal that clear FOVs can be contaminated by adjacent FOVs that lie over a different surface and which therefore have different temperatures. Coastlines are obvious examples of adjacent areas of genuinely different characteristic temperatures. Clearly we should not filter so strongly across what are known land-sea boundaries and what are therefore likely to be areas of high radiance gradient. The filtering strength is reduced by the proportion $(1 - \tau_i)$, where τ_i is the total atmospheric transmission in channel i , whenever adjacent FOVs straddle a coastline. Consequently for channels which do not sense the surface, the filtering is unchanged and for window channels the change is the greatest. The same arguments apply when filtering the bias estimate for the "MSU regression" route, and a significant part of the gain in accuracy is due to avoiding corruption to the MSU bias field rather than the to the temperature field directly.

It was noted in section 2.1 that sea and land areas have notably different characteristic variations in brightness temperature. In view of this the filtering strength is reduced over land in order not to smooth genuine features. The appropriate filtering parameter has been estimated from cleared fields of AVHRR "8" for land and sea separately and used likewise in the filter.

Improvements to error statistics with these modifications were small: 0.1 K in standard deviation and bias at most with, again, most of this coming from an improved estimate of the bias field for the "MSU regression" route.

(b) HIRS 20 albedo check

Residual contamination of "clear" FOVs is potentially very damaging on both other FOVs and on the bias field. During daytime passes, use may be made of visible channel HIRS 20. McMillin and Dean (1982) describe the use of HIRS 20 for cloud detection whereby an upper limit (threshold) for clear FOVs is set. Their threshold is stored in an historical data set updated whenever a particular earth location is found definitely clear. In NCCS a simpler approach has been adopted initially, whereby a gross threshold is set empirically after inspection of images like Figure 3a. It is set rather high so that it can detect FOVs that appear at the end of the cold "tail" but does not remove good data at the peak. Substantial errors in HIRS 8 have been avoided by use of this check. However, many FOVs are not trapped because a constant gross threshold cannot be tightened without risk of losing a lot of data. A more dynamic threshold which allows a more stringent test is being developed.

(c) Low cloud test

A well established cloud detection method with AVHRR data is a threshold on the channel 3 ($3.7\mu\text{m}$) minus channel 4 ($11\mu\text{m}$) difference (see Eyre et al. 1984). The method relies upon differing emissivities of water cloud at the two wavelengths to supply a difference in the measured brightness temperatures. It is particularly useful because low cloud often avoids other detection mechanisms (e.g. spatial coherence and infra-red thresholds). It also often avoids the estimated MSU-2 detection test because the MSU-2 weighting function is small near the surface. Following the approach used with AVHRR data, we use HIRS channels 8 ($11\mu\text{m}$) and 18 ($3.7\mu\text{m}$) and set a threshold of 2.0 K to be used at night only (since during the day solar reflection in the $3.7\mu\text{m}$ channels renders the method useless). The method is not nearly as effective within a TOVS system as it is with AVHRR data since the HIRS FOVs, being larger, are more often only partially cloud filled. Relatively few FOVs are detected by the technique but it is very fast and will be effective in a situation where large areas of low cloud are accompanied by a failure of the MSU-2 detection system due, for example, to regression biases.

(d) Other inter-channel regressions

A further attempt at residual cloud detection has been made using a technique again following AVHRR techniques and McMillin and Dean (1982). It utilises the different behaviour of the Planck function at the different wavelengths present in HIRS data. A partially cloud filled FOV will give, for channels with identical weighting functions, a higher brightness temperature in the longwave than in the shortwave because the rate of change of radiance with temperature is higher at shorter wavelengths (see, for example, Saunders 1986). Such a pair of identical channels does not exist within the TOVS system but we can take a shortwave channel, say HIRS 14, and synthesise its longwave analogue with a linear combination of channels 1-12. Typical errors in a regression relation of this sort are about 0.5 K or less. The cloud test takes an estimate of HIRS 14 from channels 1-12, whenever the FOV is supposed clear, and compares this with the measured value. If it differs by more than, say, twice the regression residual error then the FOV may be assumed to contain cloud. In practice the test is found to be rather less sensitive than the MSU-2 system and fails to identify any cloud missed by the latter.

(e) Warm biases in estimated MSU-2 values

Section 4.2 describes the problem of a warm bias in the estimated MSU-2 values used in the cloud detection. Essentially, if the estimated MSU-2 value is too high in clear FOVs then some cloudy FOVs will escape detection. This is clearly seen in Figure 11a (pass at 1307Z, 25 January 1986) over the Mediterranean. The numbers above the ellipses are (in tenths of a degree) the differences between measured and estimated MSU-2 values. This quantity has to reach a value of about +7 (= 0.7 K, the typical residual error in estimating MSU-2) before we can say with confidence that cloud is present. Figure 11a shows estimated MSU-2 values up to 2.5 K too warm in "clear" FOVs leading to a great deal of missed cloud and inaccurate values in "N*" FOVs. It would be profitable to analyse the bias, in a similar manner to the MSU-regression bias, before cloud clearing the data. If the bias estimate were reasonably accurate it would considerably improve the cloud detection.

An approach has been adopted which can currently deal only with warm biases. The only way estimated MSU-2 can be greater than measured MSU-2 is when there is both a bias error in the estimated value and little or no cloud in the FOV. The analysis is done in the following manner. The pass is divided into boxes (of about 7x7 FOVs) and a search is made of all the FOVs within a box. From the negative measured-minus-estimated MSU-2 differences, we save the one with warmest value in HIRS 8, assuming that this gives the "clearest" FOV. After examining the whole pass, the field is filtered in the normal manner to give the analysed bias. NCCS is then run normally but with the bias estimates at each FOV added to the estimated MSU-2 values. Figure 11b is equivalent to Figure 11a but with the bias correction

applied. Clear areas now have almost zero measured-minus-estimated MSU-2 differences. Detection of low cloud or small amounts of cloud is improved and N* clearances are more frequent. The impact on the pass at 1307Z on 25 January 1986, with its large biases, is substantial; the number of "clear" FOVs is halved reducing the cold "tail". The number of successful "N*" FOVs is doubled and a substantial cold bias is removed. Biases for all validated FOVs drop from 2.8 K cold to 0.4 K warm. The bias analysis scheme worked so well in this case because the biases were large and consistent. It is not expected that it will normally be so dramatic. Certainly, an extension to allow analysis of cold biases is desirable but much more difficult, since values of estimated MSU-2 which are too cold are obtained from cloud as well as from estimation errors.

Inspection of estimated MSU-2 values for other cases reveals no large biases of either sign although they may generally be expected to be present with a magnitude of the order of the residual error in the regression (about 0.7 K).

(f) Estimated errors in "N*" FOVs

NCCS uses an algorithm to calculate the expected error in an N* cleared radiance, given expected errors in the radiances used in the N* equation, in N* itself and expected correlations between these errors (see Watts 1985). However, errors in N* clearance may be dominated by the cloud field failing to satisfy the required conditions. With the AVHRR data we can test the error algorithm explicitly, comparing the estimated error with the actual error obtained from the validation. Results show a lack of any significant correlation between estimated and actual N* errors and we find this is a characteristic regardless of the correlations assumed in the estimation. This suggests errors in N* clearances are dominated by inappropriate cloud conditions and that amplification of radiometric and preprocessing noise by the N* algorithm contributes only a small part. Therefore, a complicated calculation of expected error is not justified and it seems reasonable to use an average expected error for "N*" FOVs as well as for "clear" and "MSU regression" FOVs.

5. SUMMARY

The availability of AVHRR data coincident with TOVS data permits detailed exploration and sensitive validation of the performance of a HIRS cloud-clearing scheme. We have used AVHRR data to demonstrate the improvement of the new cloud-clearing scheme (NCCS) over its predecessor, to assess the error characteristics and remaining weaknesses of the NCCS, and to make improvements to NCCS to alleviate some of the problems found.

ACKNOWLEDGMENTS

We thank our colleagues John Barnett, Philippa Lloyd and Roger Saunders for contributions to and helpful comments on this work.

REFERENCES

Aoki T.

Clear radiance retrieval of HIRS channels with the use of AVHRR data.

Tech. Proc. 1st Int. TOVS Study Conf.; 29 Aug - 2 Sept 1983; Igls, Austria; CIMSS Report, 1-9 (1984).

Eyre J.R.

High-resolution temperature retrievals at the U.K. Meteorological Office.

Tech. Proc. 1st Int. TOVS Study Conf.; 29 August - 2 Sept 1983; Igls, Austria; CIMSS Report, 94-100 (1984).

Eyre J.R.

On systematic errors in satellite sounding products and their climatological mean values.

Accepted for publication in Quart.J.Roy.Met.Soc. (1987).

Eyre J.R., Brownscombe J.L. and Allam R.J.

Detection of fog at night using AVHRR imagery.

Meteorological Magazine, 113, 266-271 (1984).

Eyre J.R. and Watts P.D.

A sequential estimation approach to cloud-clearing for satellite temperature sounding.

Submitted to Quart.J.Roy.Met.Soc. (1986).

Eyre J.R., Watts P.D., Turner J. and Lorenc A.C.

Research and development on TOVS retrievals in the U.K.

Tech. Proc. 2nd Int. TOVS Study Conf.; 18-22 February 1985; Igls, Austria; CIMSS Report, 58-74 (1985).

Lloyd P.E., Barnett J.J. and Eyre J.R.

Investigations of AVHRR data to improve TOVS retrievals.

Tech. Proc. 2nd Int. TOVS Study Conf.; 18-22 February 1985; Igls, Austria; CIMSS Report, 162-176 (1985).

McMillin L.M. and Dean C.

Evaluation of a new operational technique for producing clear radiances.

J. Appl. Meteor., 12, 1005-1014 (1982).

Saunders R.W.

An automated scheme for the removal of cloud contamination from AVHRR radiances over western Europe.

Int. J. Remote Sensing, 7, 867-886 (1986).

Smith W.L.

An improved method for calculating tropospheric temperature and moisture from satellite radiometer measurements.

Mon. Wea. Rev., 96, 387-396 (1968).

Watts P.D.

An improved TOVS cloud clearing scheme -- preliminary report.

Met. Office internal report, Met.O.19 Branch Memo 81 (1985).

Spectral Responses
AVHRR Chs. 4, 5 & HIRS Ch. 8

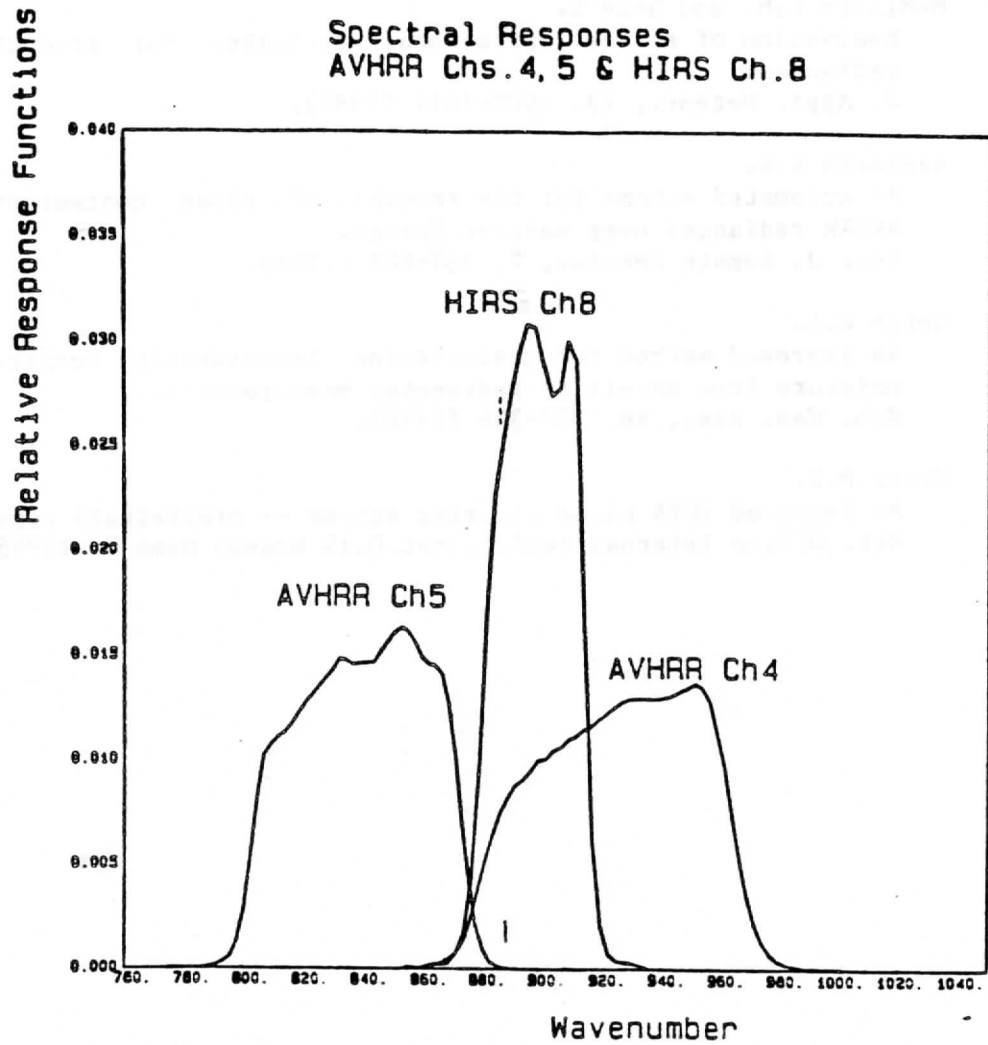


Fig. 1 Filter profiles for HIRS channel 8 and AVHRR channels 4 and 5 on NOAA-7.

HIRS AVHRR INTERCALIBRATION

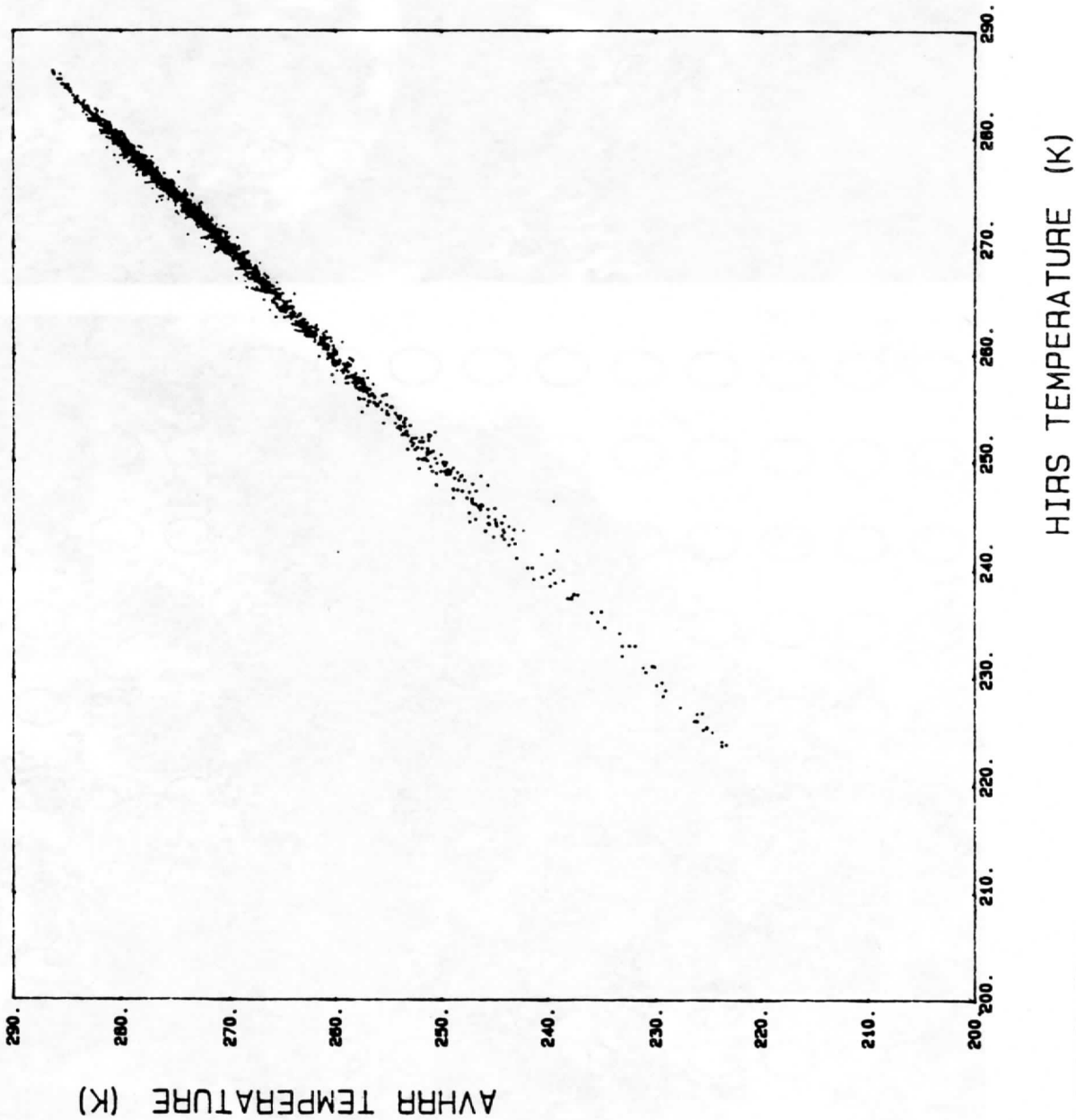


Figure 2

Illustrating the degree of agreement obtained between AVHRR "8" and HIRS 8 brightness temperatures (before cloud clearing)

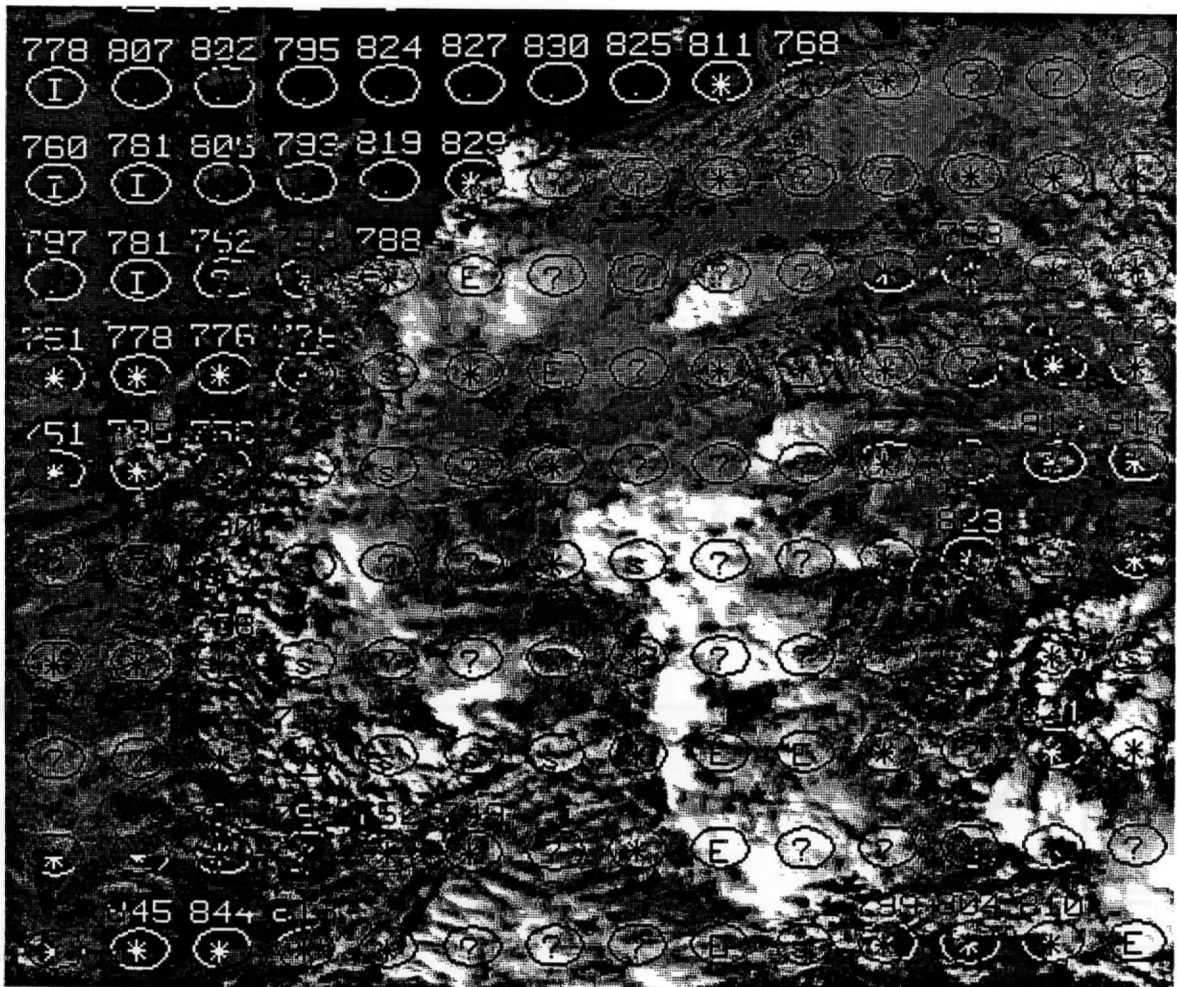


Figure 2
see text

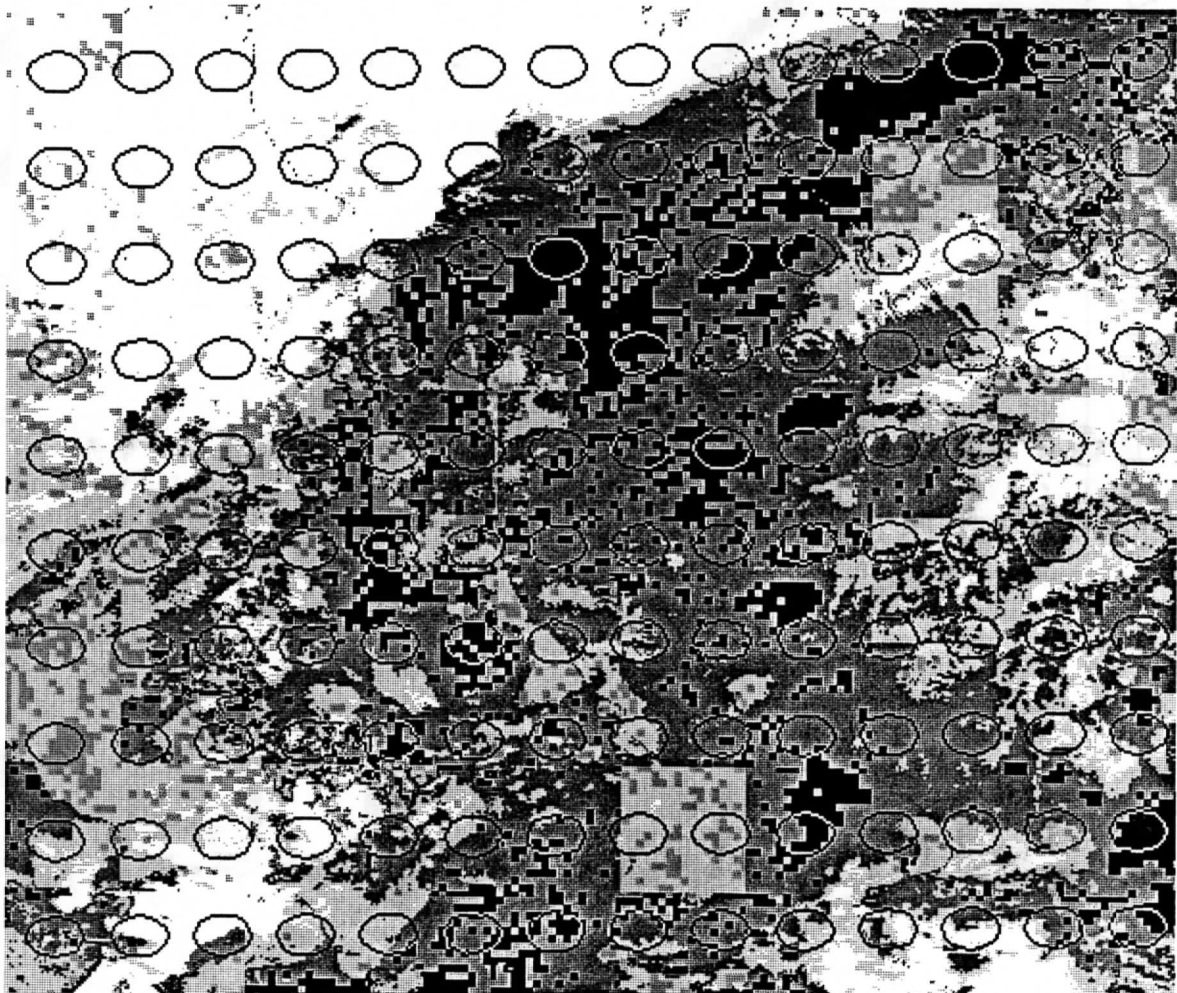


Figure 3
see text

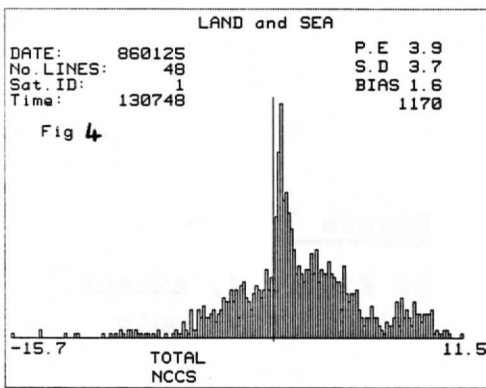


Figure 4

Histogram of AVHRR "8" minus HIRS 8 brightness temperature. NOAA-9. 25 January 1986. 1307Z. All FOVs on which AVHRR "8" values available. See text for further explanation. Data from NCCS pre-filtering.

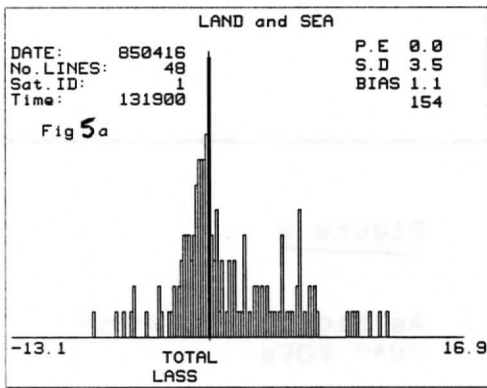


Figure 5a

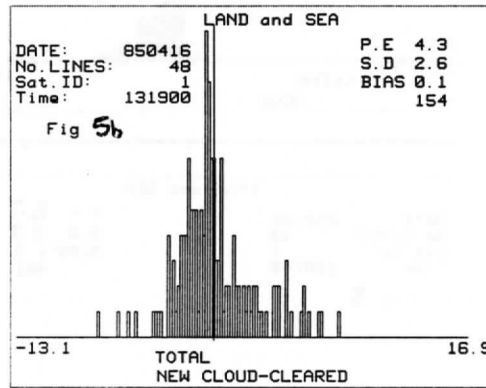


Figure 5b

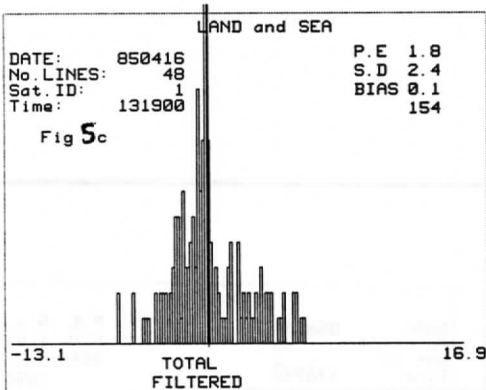


Figure 5c

As Figure 4, except for 16 April 1985 at 1319Z, and for

- (a) LASS,
- (b) NCCS pre-filtered and
- (c) NCCS post-filtered,

all for only those FOVs on which LASS values available.

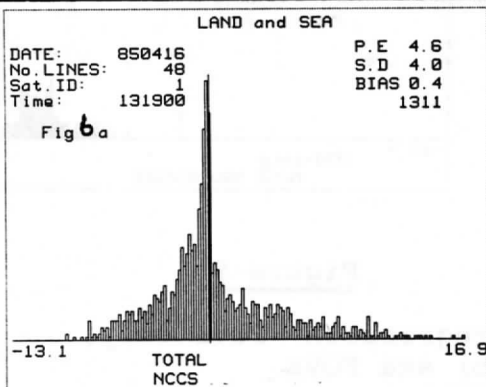


Figure 6a

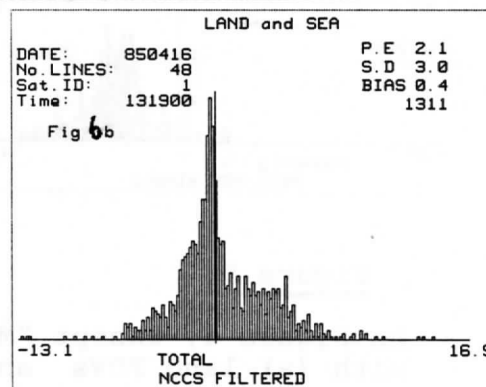


Figure 6b

As Figure 5, except for all FOVs on which NCCS values available with (a) pre-filtered and (b) post-filtered.

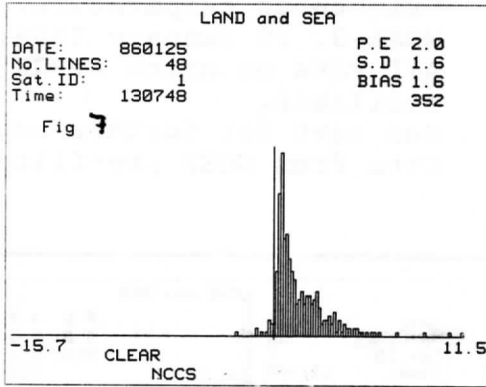


Figure 7

As Figure 4, except
"clear" FOVs only

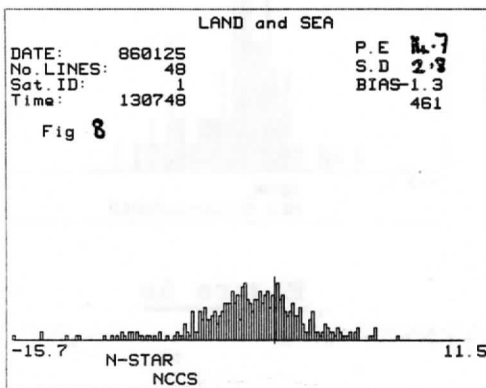


Figure 8

As Figure 4, except
"N*" FOVs

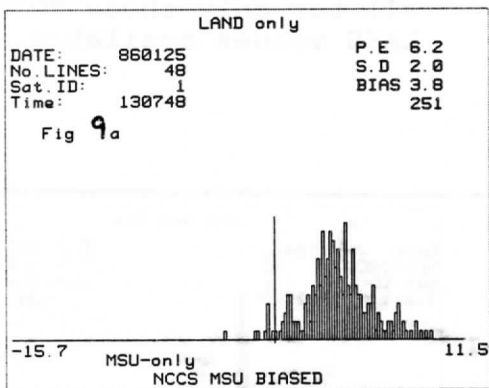


Figure 9a

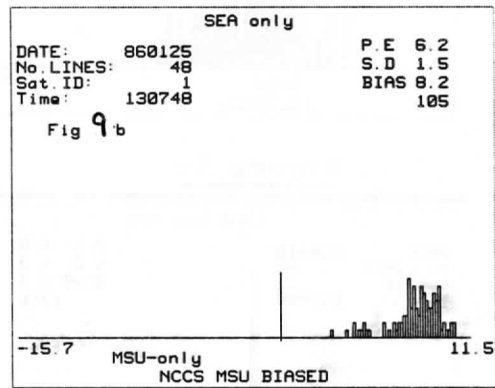


Figure 9b

As Figure 4, except "MSU regression" FOVs only,
with (a) land FOVs and (b) sea FOVs

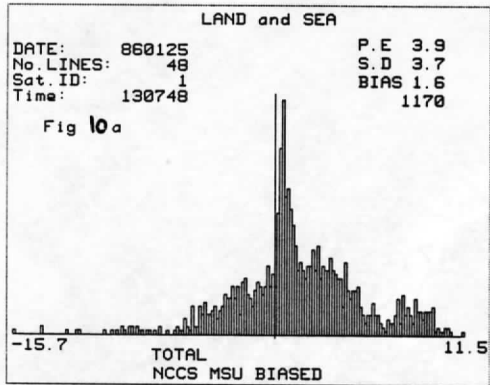


Figure 10a

As Figure 4

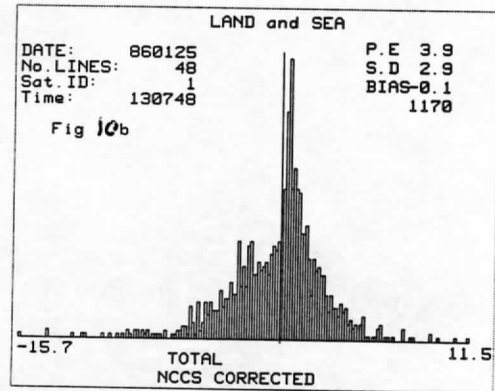


Figure 10b

As figure 4, except
after bias correction
of "MSU regression" FOVs

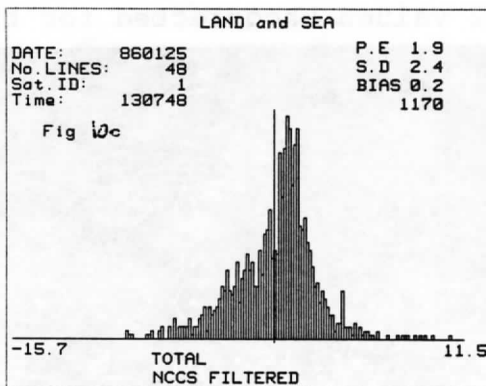


Figure 10c

As figure 4, except post-
filtering

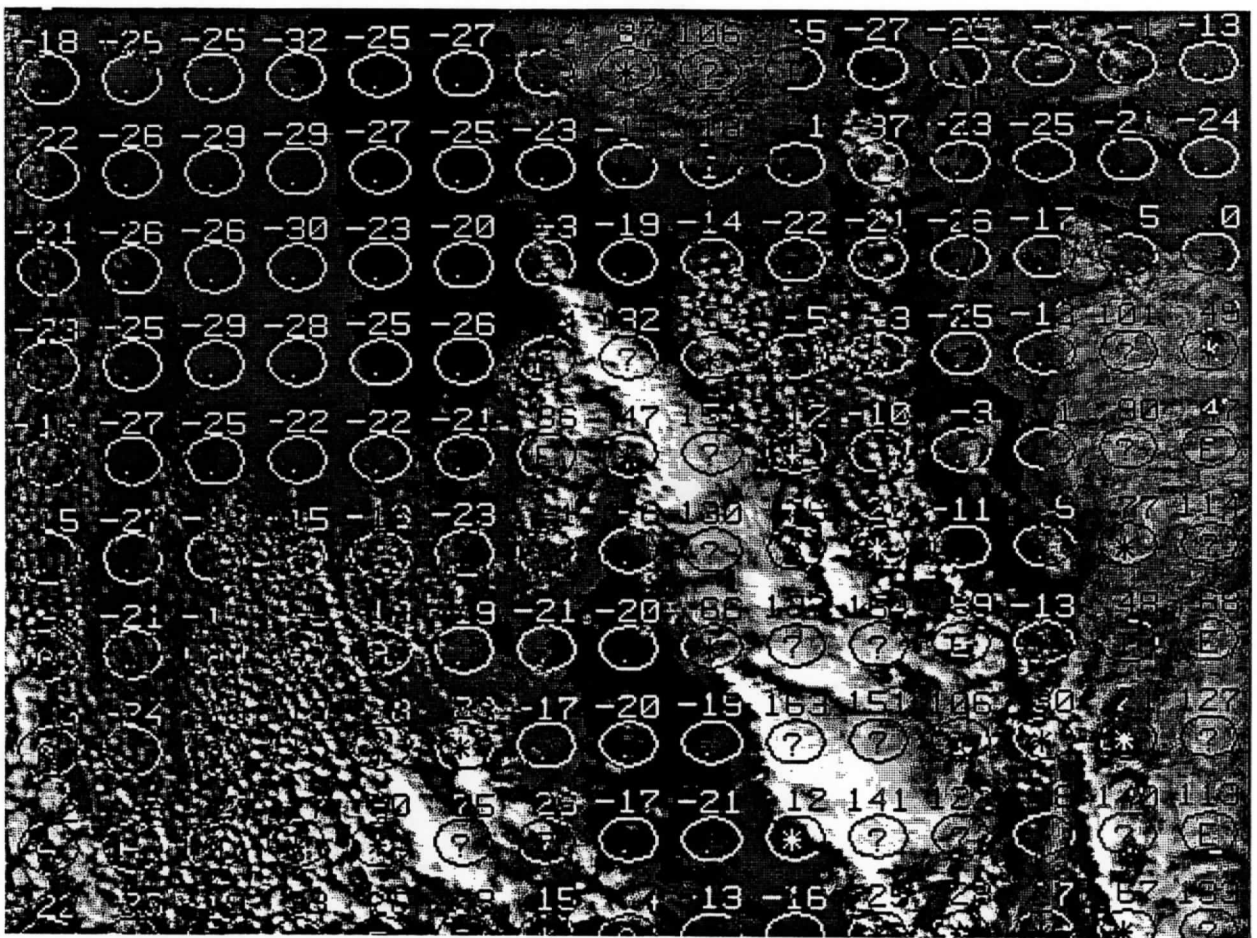


Figure 11a Estimated MSU-2 values uncorrected for bias

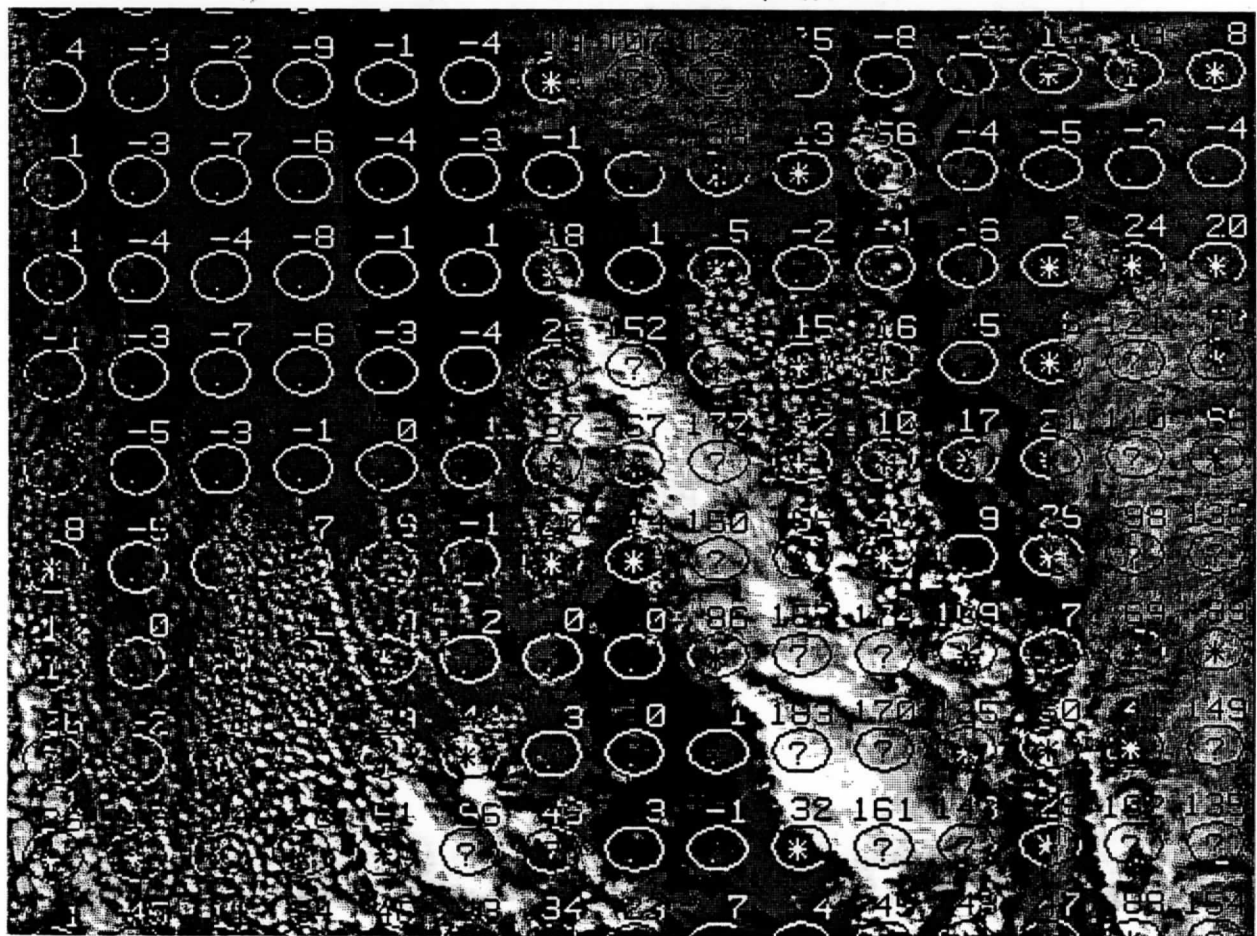


Figure 11b Estimated MSU-2 values corrected for bias

The Technical Proceedings of
The Third International TOVS Study Conference

Madison, Wisconsin

The Schwerdfeger Library
University of Wisconsin - Madison
1225 W. Dayton Street
Madison, WI 53706

August 13 - 19, 1986

Edited by

W. P. Menzel

Cooperative Institute for Meteorological Satellite Studies
Space Science and Engineering Center
University of Wisconsin
1225 West Dayton Street
Madison, Wisconsin 53706
(608) 262-0544

November 1986